Novel pharmacokinetic model to estimate dopamine dynamics in humans using PET

Dardo Tomasi (dardo.tomasi@nih.gov)
National Institutes of Health

Peter Manza
National Institutes of Health

Jean Logan
New York University

Ehsan Shokri Kojori
National Institutes of Health

Michele-Vera Yonga
National Institutes of Health

Danielle Kroll
National Institutes of Health

Dana Feldman
National Institutes of Health

Katherine McPherson
National Institutes of Health

Catherine Biesecker
National Institutes of Health

Evan Dennis
National Institutes of Health

Allison Johnson
National Institutes of Health

Kai Yuan
Xidian University

Wen-Tung Wang
National Institutes of Health

John Butman
National Institutes of Health

Gene-Jack Wang
National Institutes of Health

Nora Volkow
National Institutes of Health

Research Article

Keywords:

Posted Date: March 8th, 2022

DOI: https://doi.org/10.21203/rs.3.rs-1411479/v1

Novel pharmacokinetic model to estimate dopamine dynamics in humans using PET

Dardo Tomasi[1*], Peter Manza[1], Jean Logan[2], Ehsan Shokri-Kojori[1], Michele-Vera Yonga[1], Danielle Kroll[1], Dana Feldman[1], Katherine McPherson[1], Catherine Biesecker[1], Evan Dennis[1], Allison Johnson[1], Kai Yuan[3], Wen-Tung Wang[4], John A. Butman[4], Gene-Jack Wang[1], Nora D. Volkow[1].

[1] National Institute on Alcohol Abuse and Alcoholism, National Institutes of Health, Bethesda, Maryland, USA.

[2] Center for Biomedical Imaging, Department of Radiology, New York University School of Medicine, New York, New York, USA.

[3] School of Life Science and Technology, Xidian University, Xi'an, Shaanxi, 710071, PR China.

[4] Radiology and Imaging Sciences, Clinical Center, National Institute of Health, Bethesda, Maryland, USA.

[*]Corresponding author: Dardo Tomasi (dardo.tomasi@nih.gov), Ph.D.

Laboratory of Neuroimaging (LNI/NIAAA)

10 Center Dr, Rm B2L124

Bethesda, MD 20892-1013

Phone: (301) 496-1589

Acknowledgements

This work was accomplished with support from the National Institute of Alcohol Abuse and Alcoholism (ZIAAA000550).

ABSTRACT

Dopamine facilitates cognition and is implicated in reward processing. Methylphenidate, a dopamine enhancing medication widely used to treat attention-deficit/hyperactivity disorder, has rewarding and addictive effects if injected. Since methylphenidate's brain uptake is much faster when injected than when taken orally, we hypothesized that the amplitude and the speed of dopamine release in striatum would underly drug reward. To test this hypothesis we developed a non-invasive method to assess methylphenidate-related extracellular dopamine increases at 1-minute temporal resolution using positron emission tomography, which we validated in preclinical microdialysis data. Using a placebo-controlled double-blind within-subjects design, we show in 20 healthy controls that striatal dopamine increases induced by intravenous methylphenidate (0.25 mg/kg) were significantly faster than those induced by oral methylphenidate (60 mg) and that the time-to-peak of dopamine release was strongly associated with the intensity of self-reports of feeling "high". With this novel approach we show for the first time in humans that stronger drug reward is associated with shorter dopamine time-to-peak after methylphenidate administration.

Introduction

Dynamic measures of dopamine (DA) are needed to investigate the speed at which stimulants or other addictive drugs increase DA in striatal brain regions. The rewarding effects are much stronger when drugs are administered intravenously, presumably due to their faster brain delivery compared to when they are taken orally, which results in much slower brain uptake[1]. Dynamic striatal DA measures would also be of value for investigating the role of presynaptic DA autoreceptors (AR), which modulate DA increases by inhibiting DA release and mediating acute tolerance to the pharmacological effects of stimulant medications[2]. Current methods use position emission tomography (PET) to estimate DA release in steady-state conditions[3,4], but these models cannot account for the dynamic conditions induced by stimulants or other addictive drugs. Here, we show that a simple PET based approach allowed us to non-invasively assess the dynamics of DA increases and of autoreceptor inhibition induced by methylphenidate (MP) in the human brain, when given intravenously versus when given orally.

MP, like cocaine, blocks DA transporters (DAT)[5], thus inhibiting DA reuptake, increasing extracellular DA and occupancy of DA receptors. When MP is misused for its rewarding effects it is predominantly snorted or injected[6], which results in much faster brain delivery than when it is taken orally as is the case when used therapeutically, including attention deficit hyperactivity disorder (ADHD) treatment[7]. These different behavioral effects suggest that the rate of DA changes in brain reward regions is a crucial variable for drug reinforcement[8]. However, while this association has been inferred it has not been directly confirmed, since current strategies for measuring DA in the human brain have relied on measures that average DA changes over a 20-30 minute period[5]. Dynamic measures are needed in order to measure DA changes as they occur at

the time of peak reward and to monitor the temporal adaptations that follow DA stimulation of presynaptic AR.

To assess DA non-invasively in humans, PET methods rely on radiotracers such as [^{11}C]raclopride, which compete with endogenous DA for their binding to $D_{2/3}$ receptors and contrast their binding under baseline condition to that of interventions that increase DA[5]. Several models have been used to quantify $D_{2/3}$ receptor availability from PET data that take advantage of the minimal expression of $D_{2/3}$ receptors in cerebellum to control for non-specific binding. Here we used [^{11}C]raclopride as radiotracer and standardized uptake value ratios (SUVr) extracted from striatal and cerebellar regions to quantify DA changes induced by oral- and intravenous (IV)-MP. We hypothesized that regional reductions in standardized uptake value ratios (ΔSUVr) caused by MP would mirror cumulative extracellular DA increases relative to basal DA, $C^{DA}(t)$, in proportion to the fractional occupancy of DAT by MP, $f_{occ}^{DAT}(t)$ (e.g., larger DAT occupancy would cause smaller DA reuptake). Since DA release activates ARs to decrease the probability of release to subsequent stimulation[2], we also assumed that presynaptic AR inhibition would attenuate the rate of DA release as a function of $C^{DA}(t)$, $\eta - \alpha C^{DA}(t)$, and that the rate of clearance of extracellular DA into the intracellular compartment would be proportional to $C^{DA}(t)$ and to the availability of DAT, $1 - f_{occ}^{DAT}(t)$. Thus, the concentration of extracellular DA would be obtained by solving the ordinary differential equation:

$$\frac{dC^{DA}(t)}{dt} = \left(\eta - \alpha C^{DA}(t)\right) f_{occ}^{DAT}(t) - \beta \left[1 - f_{occ}^{DAT}(t)\right] C^{DA}(t), \qquad [1]$$

where η is the rate of DA release that reflects the firing rate of DA neurons, and α and β are the rate constants of AR inhibition and clearance of extracellular DA.

We validated this model using published microdialysis data of MP-induced striatal DA increases in the rodent and nonhuman primate brains. Then, we applied the model to test the hypothesis that the intensity of the 'high' reflects time-varying DA changes in the striatum. For this purpose, we carried out a within-subject [^{11}C]raclopride PET study with a double-blind placebo-controlled design in twenty healthy adults. We studied dynamic DA increases using oral- (slow drug brain delivery) and IV-MP (fast drug brain delivery) challenges, in association with measured subjective responses to MP using self-reports of 'high' throughout the scan.

Results

Modelling fractional occupancy of DAT

We used a 2-tissue compertment model to assess the fractional occupancy of DAT, $f_{occ}^{DAT}(t)$, in the striatum (see Methods, Eqn. [3]), assuming plasma input functions with monoexponential (IV-MP) or gamma (oral-MP) time-varying distributions (see Methods). As examples, Figs. 1A and 1B show the effects on $f_{occ}^{DAT}(t)$ of the amplitude (A) and rate constant (λ) of exponential decaying plasma MP input functions.

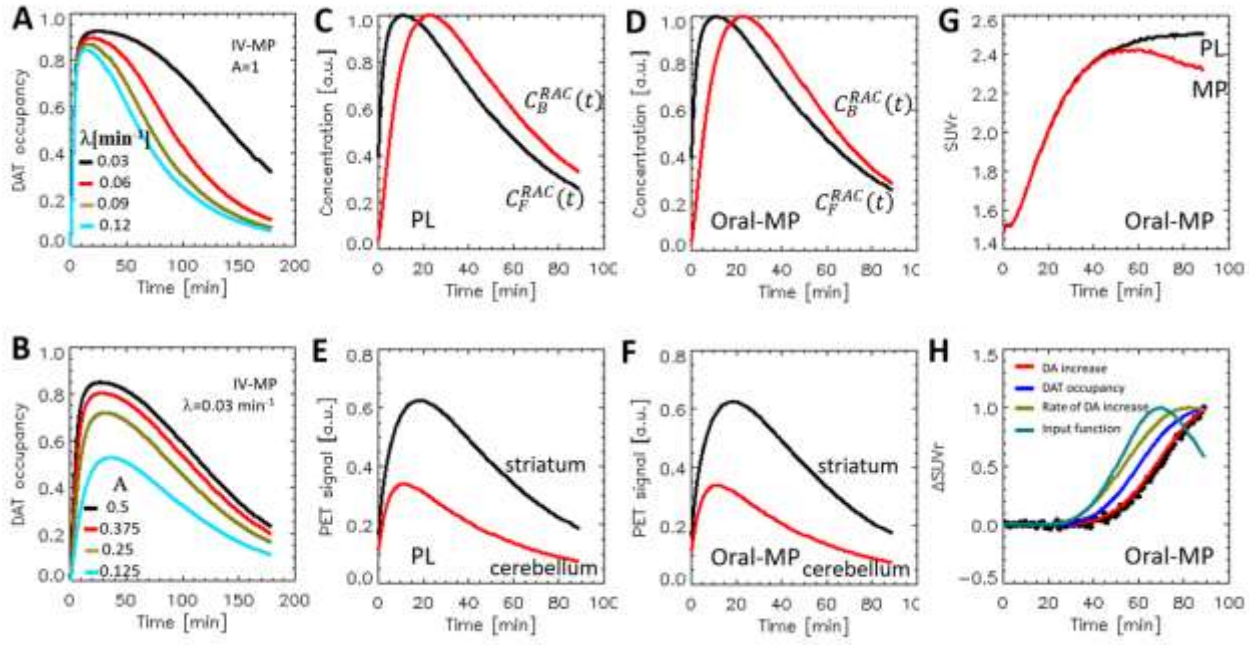

Fig 1: A and **B**: Simulations of dopamine transporter (DAT) occupancy showing that intravenous plasma methylphenidate (MP) input functions with slow decay rates (λ) were associated with more stable occupancy levels than faster decay rates, and that higher amplitudes of plasma concentration were nonlinearly associated with higher occupancy of DAT. **C** and **D**: Simulations of normalized concentrations of [11C]raclopride in free (C_F^{RAC}, black) and bound (C_B^{RAC}, red) compartments during placeblo (PL) and oral methylphenidate (MP) with added uniform random noise. **E** and **F**: Positron emission tomography signal from striatum (black) and cerebellum (red) during PL and oral-MP. **G**: Standardized uptake value ratio (SUVr) for PL and oral-MP. **H**: SUVr-difference between PL and oral-MP (ΔSUVr, black dots), dopamine (DA) increases (red), DA transporter occupancy (blue), rate of DA increases, and oral-MP input function, showing good agreement between ΔSUVr and DA increases as functions of time. K_1^{MP}=0.6 min^{-1}, k_2^{MP}=0.06 min^{-1}, k_3^{MP}=0.5 min^{-1}, and k_4^{MP}=0.2 min^{-1}; K_1^{RAC}=0.08 min^{-1}, k_2^{RAC}=0.192 min^{-1}, for a and k_3^{RAC}=k_4^{RAC}=0 (cerebellum), and K_1^{RAC}=0.15 min^{-1}, k_2^{RAC}=0.36 min^{-1}, k_3^{RAC}=0.18 min^{-1}, and k_4^{RAC}=0.05 min^{-1} (striatum). Plasma MP time-to-peak: 90 min.

Modelling the [11C]-raclopride PET signal and DA increases triggered by IV- and oral-MP challenges

To simulate time-varying PET signals in striatum and cerebellum during placebo or MP conditions (Fig 1) we used the 2-tissue compartment model (Methods Eqn [4]). The striatum-to-cerebellum signal ratio was used to simulate dynamic standardized uptake value ratios (SUVr) for placebo and MP conditions. The SUVr-difference between PL and MP conditions (ΔSUVr) demonstrated a strong correlation with DA increases caused by $f_{occ}^{DAT}(t)$, which were estimated by solving differential Eqn. [1].

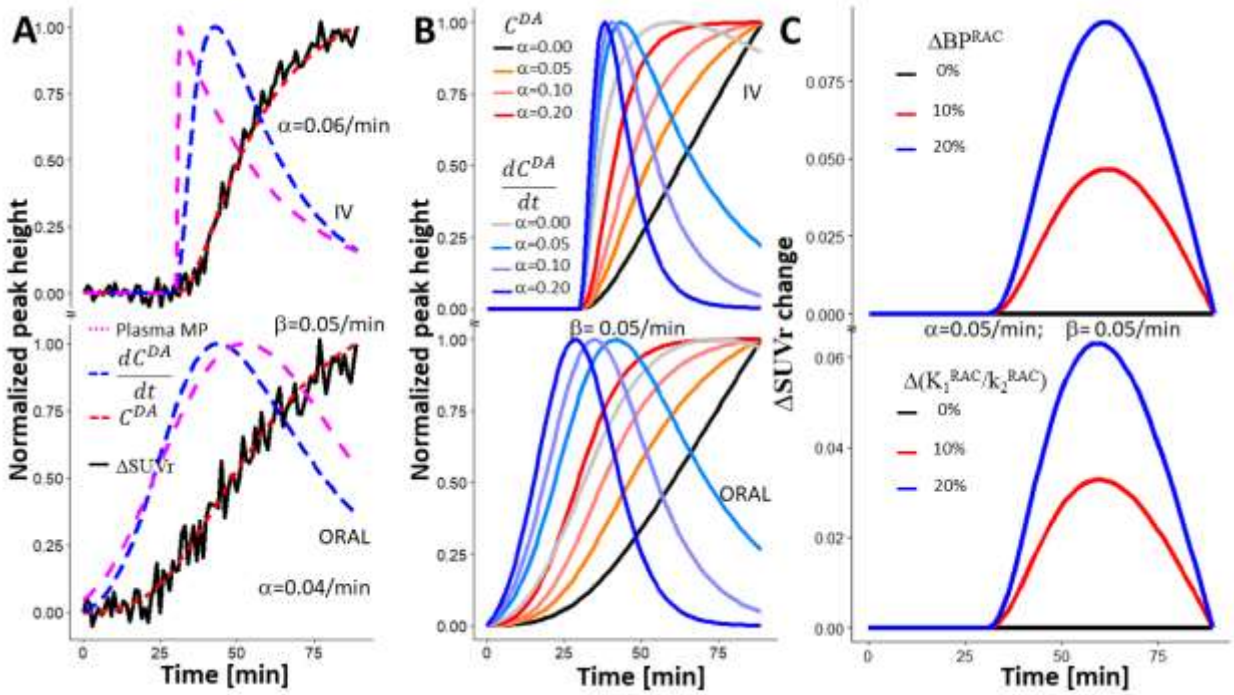

Fig 2. Simulations. A) Time-varying differences in standardized uptake value ratios (ΔSUVr; black solid line) in striatum between placebo and intravenous (IV; top) or oral (bottom) methylphenidate (MP) with added uniform random noise, and the corresponding normalized distributions of plasma MP input functions (magenta dashed lines), *apparent* DA increases (dashed red line) and its time derivative (dashed blue line). **B**) Time course of simulated DA increases and their time derivatives with different levels of autoreceptor inhibition for IV- and oral-MP. **C**) Robustness of simulated ΔSUVr to changes in binding potential ($BP^{RAC}=k_3/k_4$; top) and tissue compartment parameter ratio (K_1^{RAC}/k_2^{RAC}, bottom) for [^{11}C]raclopride. η=1. K_1^{MP}=0.6 min^{-1}, k_2^{MP}=0.06 min^{-1}, k_3^{MP}=0.5 min^{-1}, and k_4^{MP}=0.2 min^{-1}. For oral-MP, plasma MP time-to-peak=90 min. K_1^{RAC}=0.08 min^{-1}, k_2^{RAC}=0.192 min^{-1}, for a and $k_3^{RAC}=k_4^{RAC}$=0 (cerebellum), and K_1^{RAC}=0.15 min^{-1}, k_2^{RAC}=0.36 min^{-1}, k_3^{RAC}=0.18 min^{-1}, and k_4^{RAC}=0.05 min^{-1} (striatum). IV-MP injection time: 30 min. α and β are the rate constants of autoreceptor inhibition and clearance of extracellular DA.

Simulations of ΔSUVr based on a 2-tissue compartment model (see Methods) showed strong agreement with DA increases estimated via Eqn. [1] neglecting effects of AR inhibition (α=0) and DA clearance (β=0), both for IV- and oral-MP (Fig 2A). Under these conditions (α=β=0), the time derivatives of DA increases are proportional to $f_{occ}^{DAT}(t)$, which peaked at 22 and 104 minutes after the onsets of IV- and oral-MP, respectively. To estimate the effect of AR inhibition on the rate of DA release and the apparent DA increases we varied α from 0 to 0.2. These simulations demonstrated growing saturation effects on DA increases as well as earlier and narrower peaks of DA release rate with increasing α, both for oral-MP and IV-MP (Fig 2B), and the robustness of ΔSUVr to changes in [11C]raclopride pharmacokinetic parameters (Fig 2C).

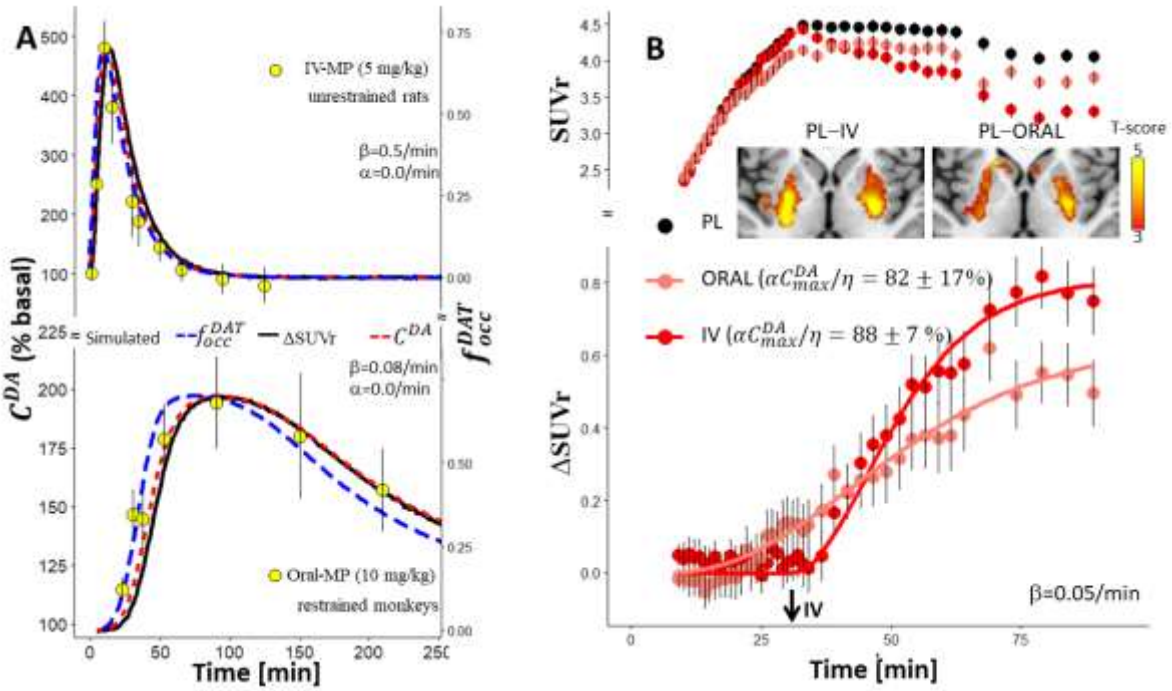

Fig 3. Dopamine (DA) increases. A) Simulated positron emission tomography (PET) data predicted dynamics of striatal extracellular DA increases measured with microdialysis after IV-MP in five unrestrained rats[9], and after oral-MP in two partially restrained awake monkeys[10]. Model parameters α and β are the autoreceptor inhibition and the DA clearance rate constants. **B**) Top: Dynamic standardized uptake value ratio (SUVr) in putamen (relative to cerebellum) for intravenous (IV), oral and placebo (PL) sessions as a function of time and statistical maps reflecting differences in non-displaceable binding potential between placebo and MP conditions, superimposed on axial views of the human brain at the level of the striatum. Bottom: dynamic DA increases, i.e. the SUVr-difference between PL and methylphenidate (MP) conditions (ΔSUVr), as a function of time. Standard error bars reflect the variability across individuals. The red (IV-MP) and pink (oral-MP) curves are model fits (Eqn.[1]). Model parameters η, α are the rates of DA release and of autoreceptor inhibition; β is DA clearance rate constant, and $\alpha C^{DA}_{max}/\eta$ is the asymptotic autoreceptor inhibition fraction. IV-MP injection time (30 min) is indicated by a down arrow. Sample for panel B: 20 healthy adults.

We validated this model against results from preclinical studies that used microdialysis to measure effects of MP on extracellular DA in striatum. Specifically, simulated ΔSUVr data predicted the average time course of DA increases measured in 5 unrestrained rats that were injected intravenously with 5 mg/kg MP[9] (χ^2=90, df=81; P=0.23), and in 2 partially restrained awake monkeys that received 10 mg/kg MP orally[10] (χ^2=42, df=36; P=0.23; Fig 3A).

MP-related DA release in the human brain

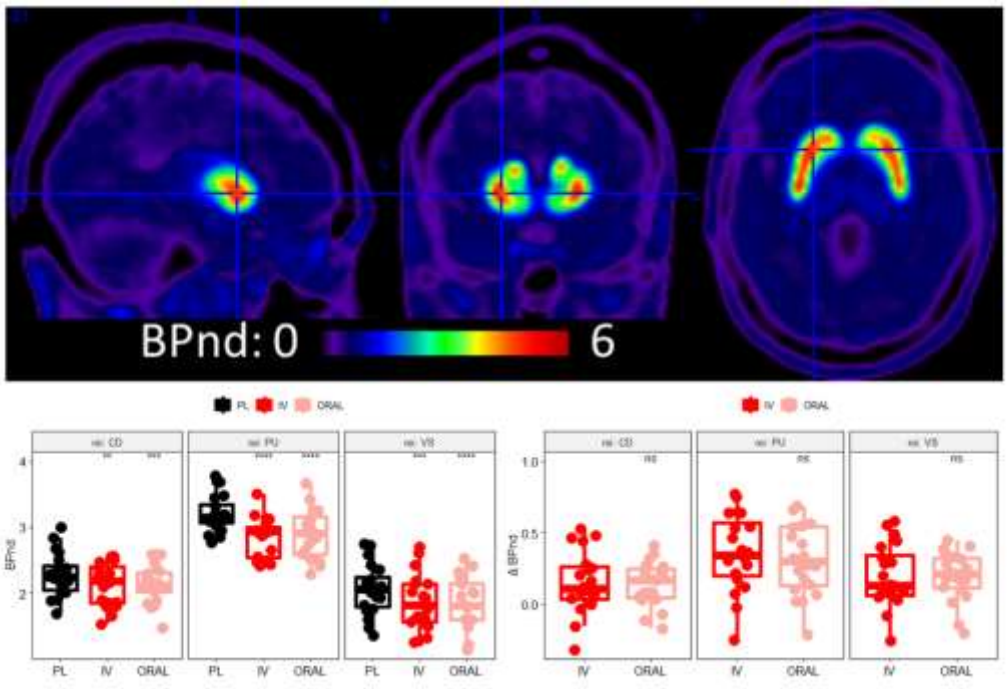

Fig 4: Binding potential. (**Top**) Spatial distribution of the non-displaceable binding potential (BPnd) in the brain of a representative individual for the placebo (PL) condition. (**Bottom**) Average BPnd values in caudate (CD), putamen (PU), and ventral striatum (VS) regions-of-interest were higher for PL than for intravenous (IV) and oral-methylphenidate (MP; left), but their differences with PL (ΔBPnd) were not significantly different between IV- and oral-MP (right). Sample: 20 healthy adults. Paired t-test comparisons against PL: ****p<0.0001; ***p<0.001; **p<0.01. Tracer: [^{11}C]raclopride.

Next, we tested our model for extracellular DA increases in 20 healthy participants (see Methods). As expected, [^{11}C]raclopride's binding was high in the striatum and low in other brain regions (Fig 4). To study the availability of $D_{2/3}$ receptors in striatum we mapped the non-displaceable binding potential (BPnd) using a graphical method that does not require blood sampling. BPnd was lower, both for IV- and oral-MP, than for placebo demonstrating significant static DA increases in striatum for the 90 min scans (P_{FWE}<0.05; Fig 3B and 4). However, the BPnd-difference between placebo and MP (ΔBPnd) was not significantly different for IV- than for oral-MP (P=0.44, F(1,85)=0.6, within-subjects ANOVA; Fig 4). These data indicate that conventional PET methods of estimating DA increases cannot capture dynamic differences in dopamine increases based on oral versus IV administration routes at the doses used here.

Speed of dopamine increases: oral versus IV MP

We estimated time-varying DA increases in putamen, caudate and ventral striatum by contrasting striatal SUVr time courses for placebo and MP conditions (Fig 3B, bottom panel). The dynamic analysis based on ΔSUVr showed significant DA increases in putamen as a function of time (P<2E-16, F(1,1835)=2524), that were higher for IV- than for oral-MP (P=0.01, F(1,1835)=6.6), and demonstrated a robust time-by-session interaction (P<5E-15, F(1,1835)=62, within-subjects ANOVA). The speed of DA increases in the striatum, estimated for 30<t<50 min using linear regression analysis, was higher for IV- (0.028±0.004 min^{-1}; mean±sd) than for oral-MP (0.011±0.003 min^{-1}; P<0.0001, t=3.6, df=19, two-sided paired t-test).

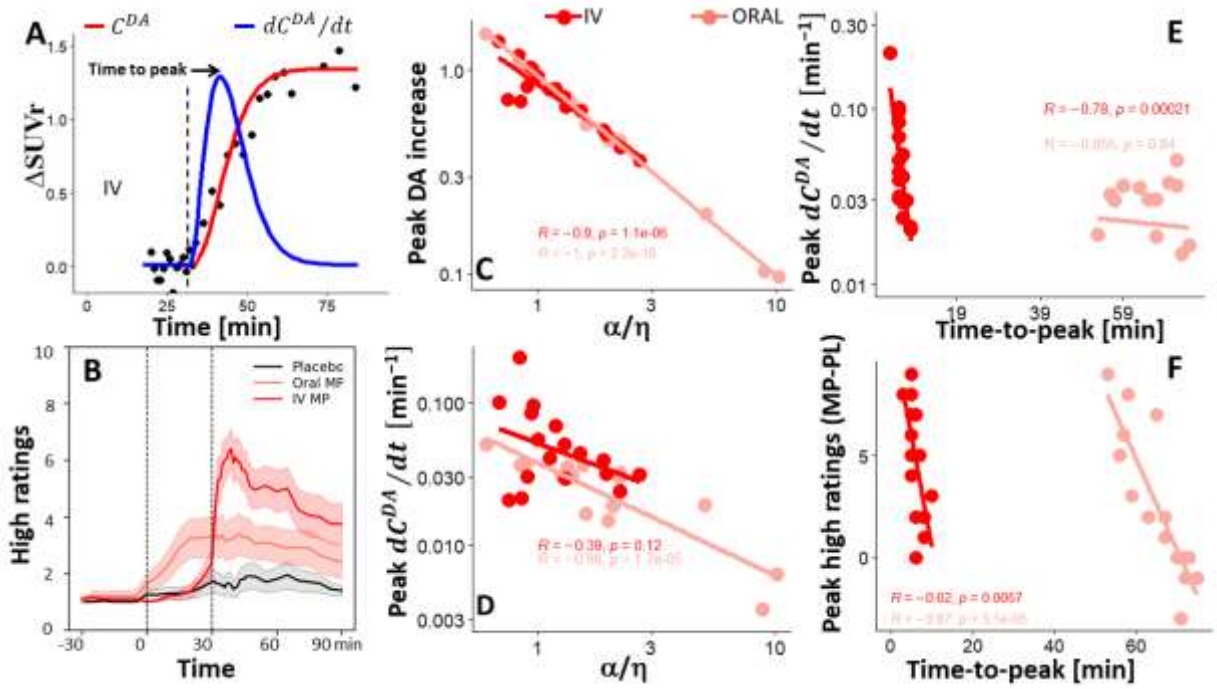

Fig 5: Interindividual variability. A) Differences in standardized uptake value ratio, ΔSUVr, between placebo (PL) and methylphenidate (MP) scans (black points), and the corresponding dopamine (DA) increases, C^{DA} (red), and their time derivatives (blue) fitted to the data for a representative individual during intravenous (IV) MP. **B**) Average high ratings across participants as a function of time. The amplitudes of DA increases (**C**) and their time derivatives (**D**) decreased with increased autoreceptor inhibition, α/η, independently for oral- and IV-MP. Model parameters α and β are the autoreceptor inhibition and clearance rate constants; η is the rate of DA release. **E**) Shorter time-to-peak was associated with higher dC^{DA}/dt amplitude during IV-MP. **F**) Linear associations between time-to-peak and differences in peak "high" ratings relative to placebo (PL), independently for oral- and IV-MP. β=0.05. Region-of-

interest: putamen. Sample: 14 (IV-MP) or 13 (Oral-MP) healthy adults. Time-to-peak was measured since the onset of MP administration (IV: 30 min, dashed line in panel A; oral: -30min). [^{11}C]raclopride was injected at t=0.

The dynamic model for the DA increases (Eqn.[1]; Fig 5A) was in good agreement with the experimental ΔSUVr(*t*) data, both for IV- and oral-MP (χ^2<2024, df>1100; P>0.08; Fig 3B, bottom panel), and revealed peak DA increases (C_{max}^{DA}) and significant effects of AR inhibition $\left(\frac{\alpha C_{max}^{DA}}{\eta} > 82\%; \text{Fig 3B}\right)$, which did not differ between oral- and IV-MP. However, there was significant variability in AR inhibition across individuals. Higher AR inhibition, α/η, in putamen was associated with lower DA increases, independently for oral- and IV-MP (R(17)<-0.9; P<1.1E-06; Figs 5C) and with lower rates of DA increases during oral-MP (R(14)=-0.88; P=1.7E-05) but not for IV-MP (Fig 5D). Higher rate of DA increase in putamen was associated with shorter time-to-peak during IV-MP (R(14)=-0.86; P<5.3E-06; Fig 5E), but not for oral-MP. Feelings of reward from MP (peak 'high' ratings; Fig 5B) were higher for IV- than for oral-MP (P=0.0002; T=4.5; df=19, paired t-test). The time-to-peak of "instantaneous DA increases" (e.g., the rate or time derivative of DA increases) in putamen was also significantly correlated with the difference in peak 'high' ratings between MP and PL (R(14)<–0.62; P<0.006, two-sided; Fig 5F).

Effect of plasma MP input function

We tested the robustness of the parametric fitting to changes in the temporal profile of the plasma MP input function for IV-MP. Specifically, for 16 healthy adults ΔSUVr(t) was fitted by Eqn [1] using different values for λ. The decay rate λ of plasma MP did not have a significant effect across subjects on η and α, C_{max}^{DA}, or time-to-peak values of the rate of DA increases (Fig 6).

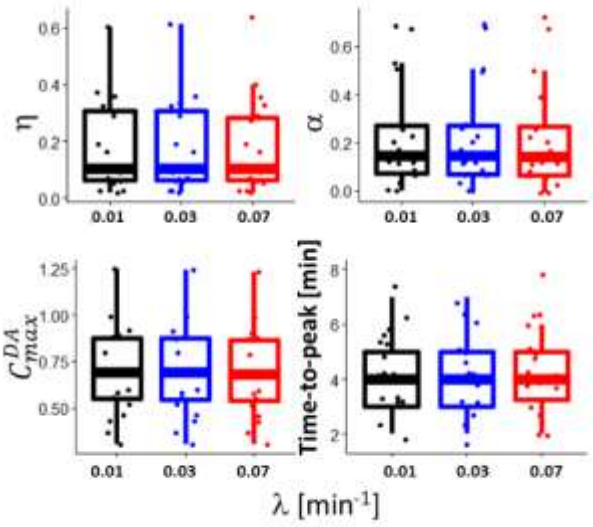

Fig 6: Effect of input function decay rate, λ. Rate of DA release, η, autoreceptor inhibition, α, peak DA accumulation, C_{max}^{DA}, and time-to-peak values obtained by fitting Eqn [1] to dynamic changes in standardized uptake value ratios (SUV) between placebo and intravenous methylphenidate for 3 different values of λ. Sample: 16 ahealthy adults.

Validation against a static metric of DA release

In striatal ROIs, static SUVr values (averaged from 30min<t<90min) were strongly correlated across participants with the distribution volume ratios (DVR; reference region: cerebellum) assessed with the Logan plot, independently for placebo, oral- and IV-MP(R(19)>0.91; P<3.3E-08; Fig 7A). SUVr- and DVR-differences between placebo and MP also exhibited high correlation across participants, independently for oral- and IV-MP (R(19)>0.84; P<3.7E-06; Fig 7B). This high correlation across subjects between the temporal average of ΔSUVr and the difference in DVR between PL and MP conditions, a standard measure of static DA increases, serves as additional experimental validation of ΔSUVr(t) as a dynamic metric of DA increases.

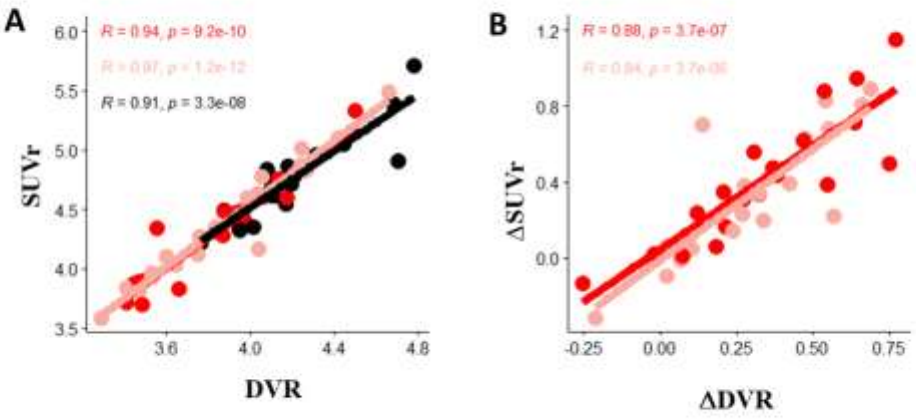

Fig 7: SUVr and DVR. **A**) Linear associations across individuals between standardized uptake value ratios (SUVr), averaged from 30min<t<90min, and distribution volume ratios (DVR) in putamen, computed using the Logan plot for intravenous (IV), oral and placebo (PL) sessions. **B**) Linear associations across individuals between MP-related SUVr and DVR decreases (ΔSUVr and ΔDVR).

Discussion

Here we propose a simple pharmacokinetic model to interpret ΔSUVr in terms of extracellular DA increases and the concomitant inhibition of DA release via AR activation. We validated this model using published microdialysis data of MP-induced striatal DA increases in rodent and nonhuman primate brains. We then applied the model to test the hypothesis that the intensity of the 'high' reflects time-varying DA changes in the striatum, using a within-subject [^{11}C]raclopride PET study with a double-blind placebo-controlled design in 20 healthy adults. We studied dynamic DA increases using oral (slow brain delivery) and IV-MP (fast brain delivery) challenges, in association with measured subjective responses to MP using self-reports of 'high'

throughout the scan and found that the time-to-peak of dopamine release was associated with the intensity of self-reports of feeling "high.

Brain dopamine (DA) signaling modulates movement, cognition, motivation, and reward[11,12]. Stimulant drugs that boost brain DA, such as methylphenidate (MP), are first-line therapeutics for disorders with abnormal DA signaling, including attention-deficit/hyperactivity disorder (ADHD)[13]. However, these stimulant medications are also widely misused for their rewarding effects, particularly when snorted or injected[8]. We had shown that DA increases induced by IV-MP were associated with measures of drug reward, but not those induced by oral-MP[7], and that the uptake of carbon-11 labeled MP ([^{11}C]methylphenidate) was associated with the short lasting duration of the "high" after IV-MP, whereas its long-lasting brain binding was not[8]. However, the interplay between dynamic DA signaling in reward circuitry and behavior is still largely unknown.

Here we developed a simple noninvasive dynamic approach to assess *apparent* DA increases at 1-minute temporal resolution. This approach, which does not require steady-state conditions as traditional methods do, relies on subtraction of SUVr(t) of [^{11}C]raclopride PET data collected with and without MP (IV and oral). Since DVR used to quantify static DA increase[14,15] have remarkable linear associations with SUVr measures[16,17], we assumed that dynamic DA increases could be quantified by SUVr(t) differences between placebo and MP scans.

The model in Eqn [1] allowed us to detect for the first time significant effects of AR inhibition on the magnitude of the DA increases triggered by MP, such that higher AR inhibition was associated with lower DA increases. This is consistent with results from preclinical studies showing that DAergic activation of AR decreases the probability of subsequent DA release, likely

to limit excess DA release during prolonged bursts of action potentials[18]. It is also consistent with MP's pharmacological effects, which by blocking DAT allow DA to accumulate depending not only on the level of DAT blockade but also on the rate at which DA is being released from the terminal[19]. To the extent that AR activation inhibits DA release this would slow down MP-induced accumulation of DA in the extracellular space[20]. Therefore, AR stimulation could cap the maximal DA increases and be a mechanism contributing to the acute tolerance observed for MP's effects[21].

The model also allowed us to document that participants with faster rates of DA increases (e.g., those for whom the time derivative of DA increases had shorter time-to-peak than 25 min after IV-MP, or 80 min after oral-MP administration) perceived the most intense 'high' during IV-MP. These findings indicate that the speed of DA increases in striatum, which is influenced by the rate of drug uptake in the brain and modualted by the route of drug administration account for why a drug like MP can be used safely for ADHD treatment orally, whereas when it is injected because it is reinforcing and can result in addiction[8,22,23]. Thus, the faster the rate of DA increases, the more intense the "high", which would also explain why very large oral doses of stimulant drugs can also be rewarding[24].

METHOD

Simulations

The time-varying concentrations of methylphenidate (MP) in the free, C_F^{MP}, and bound, C_B^{MP}, compartments were modeled using the system of ordinary differential equations:

$$\begin{cases} \dfrac{dC_F^{MP}(t)}{dt} = K_1^{MP} C_p^{MP}(t) - k_2^{MP} C_F^{MP}(t) - k_3^{MP}\left(1 - f_{occ}^{DAT}(t)\right) C_F^{MP}(t) + k_4^{MP} C_B^{MP}(t) \\ \dfrac{dC_B^{MP}(t)}{dt} = k_3^{MP}\left(1 - f_{occ}^{DAT}(t)\right) C_F^{MP}(t) - k_4^{MP} C_B^{MP}(t) \\ f_{occ}^{DAT}(t) = \dfrac{C_B^{MP}(t)}{DAT_0}, \end{cases} \quad [2]$$

where k_i^{MP} are the transfer rate constants for MP, and the fractional occupancy of DAT, $f_{occ}^{DAT}(t) = C_B^{MP}(t)/DAT_0$, depends on the total concentration of dopamine transporters, DAT_0. These equations can be expressed in terms of the relative plasma, $R^p(t) = \frac{C_p^{MP}(t)}{DAT_0}$, and free, $R(t) = \frac{C_F^{MP}(t)}{DAT_0}$, concentrations as:

$$\begin{cases} \dfrac{dR(t)}{dt} = K_1^{MP} R^p(t) - k_2^{MP} R(t) - k_3^{MP}\left(1 - f_{occ}^{DAT}(t)\right) R(t) + k_4^{MP} f_{occ}^{DAT}(t) \\ \dfrac{df_{occ}^{DAT}(t)}{dt} = k_3^{MP}\left(1 - f_{occ}^{DAT}(t)\right) R(t) - k_4^{MP} f_{occ}^{DAT}(t). \end{cases} \quad [3]$$

We assumed the following transfer rate constants for monkeys and humans[25]: K_1^{MP}=0.6 min^{-1}, k_2^{MP}=0.06 min^{-1}, k_3^{MP}=0.5 min^{-1}, and k_4^{MP}=0.2 min^{-1} (humans) or k_4^{MP}=0.05 min^{-1} (monkeys). For rats, we used K_1^{MP}=0.01 min^{-1}, k_2^{MP}=0.2 min^{-1}, consistent with microdialysis studies[26], and k_3^{MP}=0.12 min^{-1}, and k_4^{MP}=0.10 min^{-1}, consistent with a binding potential, BP=1.2[27]. For IV-MP, the simulations assumed plasma input functions, $R^p(t) = A\exp(-\lambda t)$ with $A = C_0/DAT_0$ (C_0 is the maximum plasma MP concentration that results in ~70% DAT occupancy), and λ=0.03 min^{-1} which gives a halftime of MP in blood of 23min for humans[28], or 0.30 min^{-1} that is consistent with the faster clearance of plasma MP in rats[26]. For the sake of simplicity, we ignored the fast decay component of plasma MP used in bi-exponential decay models[26]. Note that individual fits of equation [1] carried for 0.01 min^{-1}< λ<0.1 min^{-1} did not reveal significant differences in fitted

parameter (α and η), time-to-peak of DA release rate, or the maximum DA increases in striatum across subjects, suggesting that precise $R^p(t)$ modeling may not be critical for the estimation of $C^{DA}(t)$. The amplitude of its exponential decay, *A*, was fixed to 0.25 to achieve f_{occ}^{DAT}= 0.7, consistent with DAT blockade ~ 70% as documented by prior studies in humans using similar IV-MP doses[7]. Oral-MP is rapidly absorbed from the gastrointestinal tract achieving peak blood levels in 60 to 120 min[29]. Thus to model $R^p(t)$ for oral-MP, we used a probability density function of a standard gamma distribution with 90 min time-to-peak. The amplitude of the gamma probability density function for oral-MP was fixed to 10 to achieve f_{occ}^{DAT}= 0.7, as documented by prior studies in humans[7]. Since the DAT occupancy levels corresponding to the microdialisys data in rats[9] and monkeys[10] are unknown, the amplitudes of the exponential and gamma probability density functions were set as for humans.

Similarly, the time-varying concentrations of raclopride in the free, C_F^{RAC}, and bound, C_B^{RAC}, compartments can be modeled using:

$$\begin{cases} \dfrac{dC_F^{RAC}}{dt} = K_1^{RAC} C_p^{RAC}(t) - k_2^{RAC} C_F^{RAC} - k_3^{RAC}\left(1 - f_{occ}^{D23}(t)\right) C_F^{RAC} + k_4^{RAC} C_B^{RAC} \\ \dfrac{dC_B^{RAC}}{dt} = k_3^{RAC}\left(1 - f_{occ}^{D23}(t)\right) C_F^{RAC} - k_4^{RAC} C_B^{RAC}, \end{cases} \quad [4]$$

where k_i^{RAC} are the transfer rate constants for raclopride, and the fractional occupancy of $D_{2/3}$ receptors, $f_{occ}^{D23}(t) = C_B^{RAC}(t)/B_{max}$, where B_{max} is the total concentration of $D_{2/3}$ receptors. Note, that $f_{occ}^{D23}(t) \sim f_{occ}^{DAT}(t)$, since increased occupancy of DAT results in increased extracellular DA. The total concentration of the tracer, $C^{RAC}(t)$, in cerebellum and striatum was computed using $C^{RAC}(t) = (1-v)\left(C_f^{RAC}(t) + C_b^{RAC}(t)\right) + vC_p(t)$, where the blood-brain volume fraction,

ν=0.04. The concentration of the tracer in plasma was simulated as $C_p(t) = A\exp(-\lambda t)$, with A=1 and λ=0.02 min^{-1}, which is relatively consistent across human[30] and monkey[31], and λ=0.07 min^{-1} consistent with a faster clearance in rats[26,32]. For humans the transfer constants were set to K_1^{RAC}=0.08 min^{-1}, k_2^{RAC}=0.192 min^{-1}, for a and k_3^{RAC}=k_4^{RAC}=0 (cerebellum), and K_1^{RAC}=0.15 min^{-1}, k_2^{RAC}=0.36 min^{-1}, k_3^{RAC}=0.18 min^{-1}, and k_4^{RAC}=0.05 min^{-1} (striatum)[25]. For monkeys, the transfer constants were set to K_1^{RAC}=0.15 min^{-1}, k_2^{RAC}=0.192 min^{-1}, and k_3^{RAC}=k_4^{RAC}=0 (cerebellum), and K_1^{RAC}=0.55 min^{-1} and k_2^{RAC}=0.35 min^{-1}, k_3^{RAC}=0.18 min^{-1} and k_4^{RAC}=0.15 min^{-1} (striatum), consistent with a distribution volume V_D=0.76 (cerebellum) or 3.46 (striatum)[33]. For rats, the transfer rate constants were set to K_1^{RAC}=0.46 min^{-1}, k_2^{RAC}=0.41 min^{-1}, and k_3^{RAC}=k_4^{RAC}=0 (cerebellum), and K_1^{RAC}=0.46 min^{-1}, k_2^{RAC}=0.41 min^{-1}, k_3^{RAC}=0.30 min^{-1}, and k_4^{RAC}=0.50 min^{-1} (striatum)[32,34], consistent with a binding potential, BP=k_3^{RAC}/k_4^{RAC}=0.6[34].

Dynamic standardized uptake value ratios were simulated as $SUVr(t) = C_{striatum}^{RAC}(t)/C_{cerebellum}^{RAC}(t)$, and apparent cumulative DA increases (ΔSUVr) were simulated as the time-varying difference in SUVr between PL and MP. The simulations described above were implemented using the interactive data language (IDL, L3Harris Geospatial, Boulder, CO) and the Livermore solver for ordinary differential equations[35].

Studies in humans

We tested twenty healthy adults who underwent 90-min long PET scans collected in 3 randomly ordered sessions (placebo, oral-MP, and IV-MP; double-blind) while simultaneously recording their self-reported 'high' ratings (0-10) under resting conditions, using oral- and IV-MP as pharmacological challenges. In each session, each of the 20 participants was given an oral pill (60mg-MP or placebo) 30 min before injection of the PET tracer ([^{11}C]raclopride), followed 30

min after the tracer by an IV administration of 0.25mg/kg-MP or placebo. Note that these IV- and oral-MP doses led to roughly equivalent levels of DA transporter occupancy[7], and that their onsets ensured similar time-to-peak concentrations of striatal MP for oral-MP and IV-MP[8].

Participants

Twenty healthy adults (36.1±9.6 years old; 9 females) were recruited to participate in the study. All individuals provided informed consent to participate in this double-blind placebo-controlled study, which was approved by the IRB at the National Institutes of Health (Combined Neurosciences White Panel); the research was performed in accordance with all relevant guidelines and regulations. Each participant was scanned on 3 different days, 40±35 days apart, under different pharmacological conditions: 1) oral-MP (60 mg) and iv-placebo (3 cc saline), 2) oral-placebo and IV-MP (0.25 mg/kg in 3 cc sterile water), and 3) oral-placebo and iv-placebo. The session order was randomized across participants. Participants and researchers were blind to the nature of the stimulant drug (MP/PL).

PET acquisition

The participants underwent simultaneous PET/MRI imaging in a 3T Biograph mMR scanner (Siemens; Medical Solutions, Erlangen, Germany). All studies were initiated at noon to minimize circadian variability. Venous catheters were placed in the left dorsal hand vein for radiotracer injection, and in the right dorsal hand vein for intravenous injection of medications. Heart rate (HR), systolic and diastolic blood pressures (BPs) were continuously monitored throughout the study with an Expression MR400 patient monitor (Philips, Netherlands). Thirty minutes before tracer injection, either 60 mg of MP or placebo was administered p.o. The participant was then positioned in the scanner. Earplugs were used to minimize scanner noise and padding was used to minimize head motion. A T1 weighted dual-echo image was collected for

attenuation correction using an ultrashort-TE (UTE) sequence (192^3 matrix, 1.56 mm isotropic resolution, TR=11.94 ms, TE= 0.07 and 2.46 ms), and T1-weighted 3D magnetization-prepared gradient-echo (MPRAGE; TR/TI/TE = 2200/1000/4.25 ms; FA=9°, 1 mm isotropic resolution) was used to map brain structure. List mode PET emission data were acquired continuously for 90 min and initiated immediately after a manual injection of [^{11}C]raclopride as a bolus (dose =15.7±1.9 mCi; duration 5-10 seconds). Thirty minutes after tracer injection, either 0.25 mg/kg MP or placebo was manually injected i.v. as a ~30-second bolus. The participants were instructed to rest as still as possible and to relax with their eyes open during the scan.

High ratings

High rating prompts were displayed on a projector using a program (E-Prime Version 3.0) designed to minimize visual stimulation. A white cross was presented at central fixation on a black screen. Participants were instructed to stay awake, relaxed, to look at the cross, and not think of anything in particular. Occasionally, the cross would turn into a number for 10 seconds, and participants responded with a rating to the question: "How high do you feel right now, on a scale of 1-10, with 1 being minimum and 10 being maximum?". The first number presented at the start of each scanning session was always 1, and subsequent presentations matched the participant's high rating from the prior time point. Participants used a button box in their right hand to record responses. A button pressed with the right middle finger moved the rating up, one digit at a time, whereas the other button pressed with the right index finger moved the scale down. High rating prompts occurred every 5 min from the onset of oral MP administration; then, at the onset of IV-MP administration, prompts occurred every minute for 20 min –this faster sampling was chosen to capture the fast changes in reward during the first 20 min after the onset of IV-MP administration[7,36,37]; then, prompts occurred every 5 min again until the end of scanning.

MRI preprocessing

The minimal preprocessing pipelines of the Human Connectome Project (HCP)[38] were used for image processing. Specifically, FreeSurfer 5.3.0 (http://surfer.nmr.mgh.harvard.edu) was used for automatic segmentation of anatomical MRI scans into cortical and subcortical gray matter ROIs[39], and the FSL Software Library (version 5.0; http://www.fmrib.ox.ac.uk/fsl)[40] was used for spatial normalization to MNI space.

PET image reconstruction

A 3-dimensional ordered-subset expectation-maximization (OSEM) algorithm[41] with 3 iterations, 21 subsets, an all-pass filter, 344 × 344 × 127 matrix, and a model of the point spread function of the system was used for PET image reconstruction. The reconstructed PET time series consisted of 48 time windows (30 frames of 1 min, followed by 12 frames of 2.5 min, and 6 frames of 5 min) each with 2.086-mm in-plane resolution and 2.032-mm slice thickness. Attenuation coefficients (μ-maps) estimated from the UTE data using a fully convolutional neural network[42] were used to correct for scattering and attenuation of the head, the MRI table, the gantry, and the radiofrequency coil. Standardized uptake values (SUVs) for [^{11}C]raclopride were calculated after normalization for body weight and injected dose and spatially normalized to MNI space using HCP pipelines. Relative SUV time series, SUVr(t), were computed in MNI space by normalizing each SUV volume by its mean SUV in the cerebellum, as defined in individual FreeSurfer segmentations.

PET image analysis

Time-activity curves were computed for putamen, caudate, and ventral striatum and cerebellum from SUV time series using individual FreeSurfer segmentations. The Logan Plot

graphical analysis for reversible systems using the cerebellum as the reference tissue and equilibration time t*=20 min was used to map the distribution volume ratio (DVR) and non-displaceable binding potential (BPnd)[43], independently for each participant and session.

Non-linear fitting

The concentration of bound MP to DAT, $C_b^{MP}(t)$, was estimated using reported transport constants for MP[25], and the Levenberg-Marquardt algorithm for non-linear least squares fitting[44] was used to fit the model $C^{DA}(t)$ (Eqn.[1]) with 2 adjustable parameters, η and β (rats and monkeys), or η and α (humans) in IDL. For rats and monkeys α could not be modelled because of insuficient number of samples before the DA increase maxima. For human studies, since the clearance rate β could not be fitted to the data due of the lack of PET measures after t=90min, we used β=0.005 fitted in monkeys as a fixed model parameter.

Statistical analysis

Within-participants analysis of variance (ANOVA) in R was used to assess the main effects of time and session, as well as time-by-session interactions on DA increases and peak "high" ratings. χ^2 goodness-of-fit test, carried in R, was used to test how well DA(t) from Eqn [1] fitted the ΔSUVr(t) measures. We used within-participants ANOVA in the statistical parametric mapping package (SPM12; Wellcome Trust Centre for Neuroimaging, London, UK) to assess the statistical significance of BPnd in the brain. Voxelwise inference was based on a familywise error (FWE) correction for multiple comparisons[45]. Specifically, voxels were considered statistically significant if they had $P_{FWE} < 0.05$, corrected for multiple comparisons with the random field theory using a cluster defining threshold $p<0.001$.

Data availability

The datasets used during the current study available from the corresponding author on reasonable request

REFERENCES

1. Volkow, N., Fowler, J., Wang, G., Ding, Y. & Gatley, S. Role of dopamine in the therapeutic and reinforcing effects of methylphenidate in humans: results from imaging studies. *Eur Neuropsychopharmaco* **12**, 557-566 (2002).
2. Ford, C. The role of D2-autoreceptors in regulating dopamine neuron activity and transmission. *Neuroscience* **282**, 13-22 (2014).
3. Lippert, R.*, et al.* Time-dependent assessment of stimulus-evoked regional dopamine release. *Nat Commun* **10**, 336 (2019).
4. Thanarajah, S.*, et al.* Food Intake Recruits Orosensory and Post-ingestive Dopaminergic Circuits to Affect Eating Desire in Humans. *Cell Metab* **29**, 695-706 (2019).
5. Volkow, N.*, et al.* Is methylphenidate like cocaine? Studies on their pharmacokinetics and distribution in the human brain. *Arch Gen Psychiatry* **52**, 456-463 (1995).
6. Klein-Schwartz, W. Abuse and toxicity of methylphenidate. *Curr Opin Pediatr* **14**, 219-223 (2002).
7. Volkow, N.*, et al.* Dopamine transporter occupancies in the human brain induced by therapeutic doses of oral methylphenidate. *Am J Psychiatry* **155**, 1325-1331 (1998).
8. Volkow, N. & Swanson, J. Variables that affect the clinical use and abuse of methylphenidate in the treatment of ADHD. *Am J Psychiatry* **160**, 1909-1918 (2003).
9. Aoyama, T., Kotaki, H., Sawada, Y. & Iga, T. Pharmacokinetics and pharmacodynamics of methylphenidate enantiomers in rats. *Psychopharmacology (Berl)* **127**, 117-122 (1996).
10. Kodama, T.*, et al.* Oral Administration of Methylphenidate (Ritalin) Affects Dopamine Release Differentially Between the Prefrontal Cortex and Striatum: A Microdialysis Study in the Monkey. *J Neurosci* **37**, 2387-2394 (2017).
11. Arnsten, A. Catecholamine regulation of the prefrontal cortex. *J Psychopharmacol* **11**, 151-162 (1997).
12. Volkow, N., Wise, R. & Baler, R. The dopamine motive system: implications for drug and food addiction. *Nat Rev Neurosci* **18**, 741-752 (2017).
13. Faraone, S. The pharmacology of amphetamine and methylphenidate: Relevance to the neurobiology of attention-deficit/hyperactivity disorder and other psychiatric comorbidities. *Neurosci Biobehav Rev* **87**, 255-270 (2018).
14. Volkow, N.*, et al.* Reinforcing effects of psychostimulants in humans are associated with increases in brain dopamine and occupancy of D(2) receptors. *J Pharmacol Exp Ther* **291**, 409-415 (1999).
15. Volkow, N.*, et al.* Therapeutic doses of oral methylphenidate significantly increase extracellular dopamine in the human brain. *J Neurosci* **21**, RC121 (2001).
16. Lockhart, S.*, et al.* Dynamic PET Measures of Tau Accumulation in Cognitively Normal Older Adults and Alzheimer's Disease Patients Measured Using [18F] THK-5351. *Plos ONE* **11**, e0158460 (2016).
17. O'Dell, R.*, et al.* Validation of a simplified tissue-to-reference ratio measurement using SUVR for the assessment of synaptic density alterations in Alzheimer's disease using [11C]UCB-J PET. *Alzheimer's Dement* **16**, e045928 (2020).
18. Benoit-Marand, M., Borrelli, E. & Gonon, F. Inhibition of dopamine release via presynaptic D2 receptors: time course and functional characteristics in vivo. *J Neurosci* **21**, 9134-9141 (2001).

19. Volkow, N.*, et al.* Relationship between blockade of dopamine transporters by oral methylphenidate and the increases in extracellular dopamine: Therapeutic implications. *Synapse* **43**, 181-187 (2002).
20. Seeman, P. & Madras, B. Anti-hyperactivity medication: methylphenidate and amphetamine. *Mol Psychiatry* **3**, 386-396 (1998).
21. Swanson, J.*, et al.* Acute tolerance to methylphenidate in the treatment of attention deficit hyperactivity disorder in children. *Clin Pharmacol Ther* **66**, 295-305 (1999).
22. Verebey, K. & Gold, M. From coca leaves to crack: the effects of dose and routes of administration in abuse liability. *Psychiatr Annals* **18**, 513-520 (1988).
23. Zweifel, L.*, et al.* Disruption of NMDAR-dependent burst firing by dopamine neurons provides selective assessment of phasic dopamine-dependent behavior. *Proceedings of the National Academy of Sciences U S A* **106**, 7281-7288 (2009).
24. Morton, W. & Stockton, G. Methylphenidate Abuse and Psychiatric Side Effects. *Prim Care Companion J Clin Psychiatry* **2**, 159-164 (2000).
25. Logan, J.*, et al.* A strategy for removing the bias in the graphical analysis method. *J Cereb Blood Flow Metab* **21**, 307-320 (2001).
26. Aoyama, T., Yamamoto, K., Kotaki, H., Sawada, Y. & Iga, T. Pharmacodynamic modeling for change of locomotor activity by methylphenidate in rats. *Pharm Res* **14**, 1601-1606 (1997).
27. Sossi, V.*, et al.* In vivo dopamine transporter imaging in a unilateral 6-hydroxydopamine rat model of Parkinson disease using 11C-methylphenidate PET. *J Nucl Med* **53**, 813-822 (2012).
28. Ding, Y.*, et al.* Chiral drugs: comparison of the pharmacokinetics of [11C]d-threo and L-threo-methylphenidate in the human and baboon brain. *Psychopharmacology (Berl)* **131**, 71-78 (1997).
29. Markowitz, J.*, et al.* Pharmacokinetics of methylphenidate after oral administration of two modified-release formulations in healthy adults. *Clin Pharmacokinet* **42**, 393-401 (2003).
30. Sestini, S., Halldin, C., Mansi, L., Castagnoli, A. & Farde, L. Pharmacokinetic Analysis of Plasma Curves Obtained After i.v. Injection of the PET Radioligand [11C] Raclopride Provides a Likely Explanation for Rapid Radioligand Metabolism. *J Cell Physiol* **227**, 1663-1669 (2012).
31. Tsukada, H.*, et al.* Ketamine decreased striatal [(11)C]raclopride binding with no alterations in static dopamine concentrations in the striatal extracellular fluid in the monkey brain: multiparametric PET studies combined with microdialysis analysis. *Synapse* **37**, 95-103 (2000).
32. Wong, Y., Trayana Ilkova, T., van Wijk, R., Hartman, R. & de Lange, E. Development of a population pharmacokinetic model to predict brain distribution and dopamine D2 receptor occupancy of raclopride in non-anesthetized rat. *Eur J Pharm Sci* **111**, 514-525 (2018).
33. Carson, R.*, et al.* Quantification of amphetamine-induced changes in [11C]raclopride binding with continuous infusion. *J Cereb Blood Flow Metab* **17**, 437-447 (1997).
34. Hume, S.*, et al.* Quantitation of carbon-11-labeled raclopride in rat striatum using positron emission tomography. *Synapse* **12**, 47-54 (1992).
35. Hindmarsh, A. LSODE and LSODI, two new initial value ordinary differnetial equation solvers. *ACM SIGNUM Newsletter* **15**, 10-11 (1980).
36. Volkow, N.*, et al.* Cardiovascular effects of methylphenidate in humans are associated with increases of dopamine in brain and of epinephrine in plasma. *Psychopharmacology (Berl)* **166**, 264-270 (2003).
37. Volkow, N.*, et al.* Temporal relationships between the pharmacokinetics of methylphenidate in the human brain and its behavioral and cardiovascular effects. *Psychopharmacology (Berl)* **123**, 26-33 (1996).
38. Glasser, M.*, et al.* The minimal preprocessing pipelines for the Human Connectome Project. *Neuroimage* **80**, 105-124 (2013).

39. Fischl, B.*, et al.* Whole brain segmentation: automated labeling of neuroanatomical structures in the human brain. *Neuron* **33**, 341-355 (2002).
40. Smith, S.*, et al.* Advances in functional and structural MR image analysis and implementation as FSL. *Neuroimage* **23 suppl 1**, S208-S219 (2004).
41. Hudson, H. & Larkin, R. Accelerated image reconstruction using ordered subsets of projection data. *IEEE Trans Med Imaging* **13**, 601-609 (1994).
42. Roy, S., Butman, J. & Pham, D. Synthesizing CT from Ultrashort Echo-Time MR Images via Convolutional Neural Networks. in *Simulation and Synthesis in Medical Imaging* (eds. Tsaftaris, S., Gooya, A., Frangi, A. & Prince, J.) 22-32 (Springer Nature, Quebec, Canada, 2017).
43. Logan, J.*, et al.* Graphical analysis of reversible radioligand binding from time-activity measurements applied to [N-11C-methyl]-(-)-cocaine PET studies in human subjects. *Journal of Cerebral Blood Flow and Matabolism* **10**, 740-747 (1990).
44. Press, W., Teukolsky, S., Vetterling, W. & Flannery, B. *Numerical Recipes in C. The Art of Scientific Computing*, (Cambridge University Press, New York, 1992).
45. Eklund, A., Nichols, T. & Knutsson, H. Cluster failure: Why fMRI inferences for spatial extent have inflated false-positive rates. *Proc Natl Acad Sci U S A.* **113**, 7900-7905 (2016).